Modeling of Leaching Filter Pressure Drop and Fouling Behavior – 10477

D.R. Rector and M.L. Stewart
Pacific Northwest National Laboratory
P.O. Box 999, Richland, WA

ABSTRACT

A new simulation capability has been developed for modeling the flow and thermal performance of chemical processes that involve multiphase, chemically-complex flows. This capability is applied to the ultrafiltration process which will be used in conjunction with caustic and/or oxidative leaching to concentrate high level waste in the Waste Treatment and Immobilization Plant (WTP) at the US DOE Hanford site. The separation of supernatant from undissolved solids is an important aspect of these processes. The design and likely operational performance of the proposed ultrafiltration system for the WTP facility have been called into question by external reviewers. In this work, lattice methods are used to model both the pore scale filtration mechanisms in the filter material and the filter device scale performance. Simulation results are compared with data from experiments.

INTRODUCTION

Designing high-level waste processing facilities depends heavily on the ability to scale the fundamental processes developed during bench tests to a full sized plant. For this reason, a general simulation capability has been developed for modeling the flow and thermal performance of chemical processes that involve multiphase, chemically complex flows of a potentially non-Newtonian nature. This capability is designed to take advantage of new high performance computing systems with large numbers of parallel processers. We plan to further demonstrate this capability in the future by applying it to a series of chemical processing applications.

The application described here involves the pretreatment of high-level waste at the DOE Office of River Protection's Waste Treatment Plant (WTP), which includes the separation of aluminum compounds through caustic leaching. An important aspect of this process is the separation of supernatant from undissolved solids through ultrafiltration. Significant potential issues with the proposed leaching processes and associated ultrafiltration system were identified by a panel of external experts [1]. In response to their concerns the Pretreatment Engineering Platform (PEP) was constructed and operated by PNNL to verify the effectiveness of several aspects of the WTP design. As part of this effort, a series of experiments were performed to assess the filter performance [2].

The filter unit consists of a series of sintered stainless steel tubes which are operated as crossflow filters, where the slurry is pumped through the center of the tubes at a specified rate and the filtrate passes through the tube wall and is collected in the region surrounding the tubes. A conceptual model of the filter process is shown in Figure 1. The filter flux for a specified trans-membrane pressure drop is affected by the flow resistance of the tube filter media, the fine

particles embedded in the filter media and the filter cake that grows on the inside surface of the filter tube. The slurry cross flow creates a shear stress at the surface of the filter which acts to minimize the accumulation of filter cake.

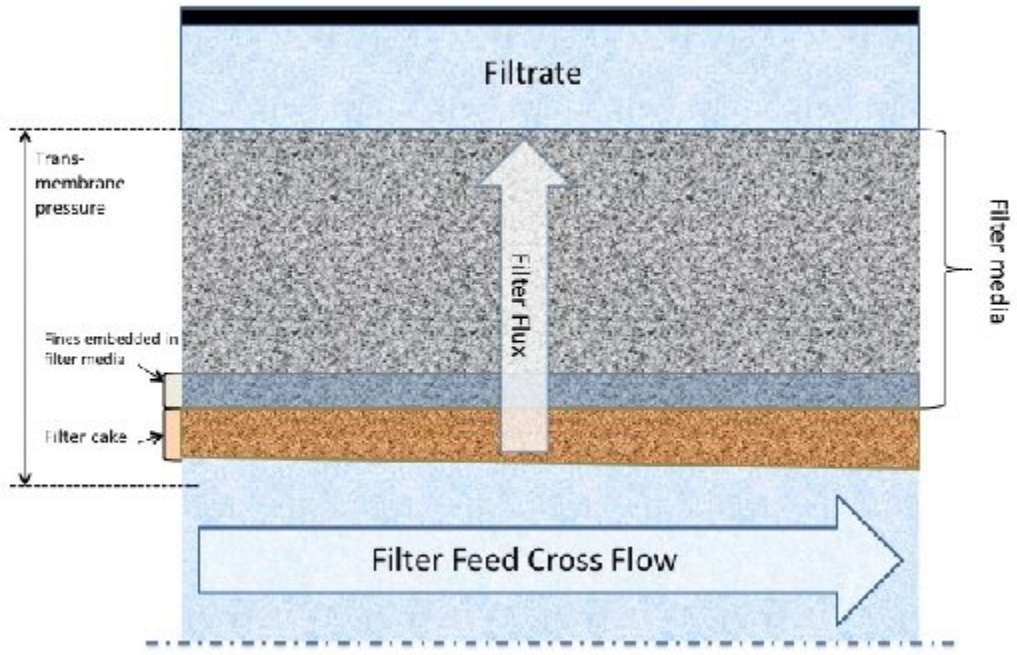

Figure 1. Conceptual model of filter

Efficient operation of the filter requires maintaining a reasonable filtrate flux rate for a given pressure drop across the filter and filter cake, which depends on the degree of fouling within the filter. Excessive fouling requires frequent backwash and cleaning, which delays waste plant production and reduces throughput.

A significant amount of work has been done to develop models for the ultrafiltration of Hanford waste, including dewatering and sodium removal from waste feed [3-5] and, more recently, the ultrafiltration used in conjunction with the leaching process. The approach taken is to develop an expression for the filter flux rate using composite coefficients for the effective mass transfer for shear-induced back transport and for filter resistance. The work described in this paper uses a different but complimentary modeling approach that examines in more detail the particle capture behavior in the filter was well as the effect of shear on the polydisperse concentration profile above the filter surface which in turn has a significant effect on filter cake growth.

SIMULATION METHOD

Filter modeling is challenging because the macroscopic device-scale filter performance depends on pore-scale particle capture and corresponding changes in the flow and pressure fields in the filter material. For this reason, computational models were developed at two different scales to

address pressure drop and fouling behavior. We first describe a pore-scale model which was developed to examine the mechanisms leading to "deep bed filtration" fouling. The results from the pore-scale model are then used to develop constitutive relationships for use in a device scale model which was developed to predict the performance of the filtration unit as a function of time.

Pore Scale Model

A stochastic reconstruction technique was used to generate the digital geometry representing the filter pore structure. Individual grain shapes were placed randomly in a three-dimensional volume in an arrangement similar to that of the sintered material making up the actual filters. Selection of the size and shape of the constituent grains was informed by micrographs. Grains may be overlapped within a specified range, small cracks and voids may be filled, or features such as sharp corners and narrow throats may be eroded as required in order to make the reconstructed geometry more realistic. Key material parameters to match are porosity and average pore size. If a greater level of fidelity is required, statistical metrics such as chord length distributions or two-point correlations may be used to match the reconstruction to the real material.

The lattice-Boltzmann (LB) method is used to calculate the flow field through the filter pore structure. The LB method has been widely used for flow field simulations in porous media because its inherent parallelism allows the solution of complex flow fields to be shared among large numbers of processors, allowing solutions in reasonable wall clock times. The LB method has also been used by a number of researchers for simulation of the filtration process [6-9]. Although lattice-Boltzmann is used in the micro-scale filtration simulation presented here, all of the techniques discussed are also fully compatible with the lattice kinetic technique currently under development at PNNL.

In the work discussed here, filtration is simulated using Lagrangian particle tracking. Individual particles are introduced at the upstream boundary and carried by the flow field toward the filter wall. Particle motion is determined by fluid dynamic forces, particle momentum, and random Brownian effects. Simple Euler integration is used to track particle paths. Deposition of particles may occur when they contact a wall surface or a previously deposited particle. A sticking probability may be specified to determine whether a given contact leads to particle immobilization, or sticking can be made a function of particle momentum or the local shear in the fluid flow field. If a particle makes contact with an obstruction but is not captured, hard sphere recoil is assumed. A Darcy resistance to flow is introduced in cells where particles deposit, which allows the flow field to evolve in a realistic manner as filtration takes place. The Kuwabara model[10,11] is used to estimate the filter cake permeability from particle size and porosity. While it would be possible in principal to conduct particle tracking simulations with particles having various sizes and shapes, the simulations discussed here assume spherical particles with a diameter of 300 nanometers. Unit collector filtration theory [12] suggests that particles of roughly this size can be expected to penetrate the deepest into the filter walls, and therefore present the most danger of fouling. This particle size is on the small end of the size distribution observed for waste stimulants used in the PEP tests before leaching operations, but particles in this size range would be more abundant after leaching.

Device Scale Model

The computational resources required for the pore scale model limit the size of domain that can be modeled. The device scale model was developed to predict the performance of the filtration unit as a function of time. The spatial domain is subdivided into nodes or lattice sites that represent the tube channel or porous wall regions. The filter medium is modeled as a continuum with specified properties such as flow resistances and capture efficiencies. The information obtained from the pore scale model is reduced to create constitutive relationships for these composite properties. Initial flow rate, v, through the porous media regions can be expressed as

$$v = \frac{\nabla P}{\mu R} \qquad \text{(Eq. 1)}$$

where μ is the liquid viscosity and R is the Darcy resistance.

The particle size distribution is divided into a limited number of particle size bins with an associated transport equation for each size bin. A significant fraction of the particle size distribution is larger than the average pore size. As the filtrate flux draws particles to the membrane surface, the larger particles will accumulate and increase the solids concentration near the surface while the smaller particles will enter the pores.

As particles move through the sintered filter material, they become trapped due to pore constrictions and particulate deposits or due to surface forces. Separate continuum fields are used to represent solids deposited in the filter from each size bin. The rate of deposition is an expression based on local concentration, deposited solids and flow rate

$$\frac{d\phi_{i,dep}}{dt} = k_i \phi_i f(v, \phi_i, \phi_{dep}) \qquad \text{(Eq. 2)}$$

where k is the capture coefficient, ϕ is the total suspended solids volume fraction (cm^3 solids/ cm^3), ϕ_i is the solids volume fraction for suspended particles in size bin i, ϕ_{dep} is the total volume fraction of deposited solids, and $\phi_{i,dep}$ is the solids volume fraction for deposited particle in size bin i.

The particle suspension near the surface of the filter membrane is sheared, resulting in a shear-driven migration of particles back toward the center of the channel. This is due to the asymmetric number of particle collisions and momentum transfer in the transverse direction when there is a concentration gradient. The back particle flux for a uniform particle system is [13]

$$J_b = -D(\phi)\dot{\gamma} a^2 \phi^2 \frac{d\phi}{dz} \qquad \text{(Eq. 3)}$$

where a is the particle diameter, ϕ is the solids volume fraction, γ is the local shear rate and D is

a dimensionless diffusion coefficient that is a function of solids volume fraction. A more general form for particle size i of a polydisperse suspension was developed by Shauly et al. [14,15]

$$J_i = -\dot{\gamma}\left[k_c a_i \left(\sum_j a_j \phi_j \right) \nabla \phi_i + k_\mu \bar{a}^2 \phi \phi_i \frac{1}{\mu} \nabla \mu \right] \qquad \text{(Eq. 4)}$$

where a is the average particle diameter, ϕ_i is the solids volume fraction for particle size i and μ is the effective viscosity. The Krieger expression is used for calculating the suspension viscosity [16]

$$\mu = \mu_0 \left(1 - \frac{\phi}{\phi_m} \right)^{-n} \qquad \text{(Eq. 5)}$$

where ϕ_m is the maximum packing density and μ_0 is the liquid viscosity.

The suspension concentration increases at the filter surface and a concentration profile develops, also known as concentration polarization. The profile is determined by the rate of particle transport toward the surface due to the filtration flux and the shear-induced back-transport. The back-transport flux creates an additional filtrate flow resistance in the transverse direction.

The shear-induced migration will also affect the suspended particle size composition near the filter surface. The flux rate for individual particle sizes in Equation 4 increases as a function of particle diameter. Therefore, the larger particles preferentially migrate toward the center of the channel.

Turbulent quantities in the tube channel are calculated using a k-epsilon RANS (Reynolds-averaged Navier-Stokes) model. The transport equations for the turbulent energy, k, and dissipation, ε, are

$$\frac{\partial k}{\partial t} + U_j \frac{\partial k}{\partial x_j} = \frac{\partial}{\partial x_j} \left[\left(\nu + \frac{\nu_T}{\sigma_k} \right) \frac{\partial k}{\partial x_j} \right] + \tau_{ij} \frac{\partial U_i}{\partial x_j} - \varepsilon \qquad \text{(Eq. 6)}$$

$$\frac{\partial \varepsilon}{\partial x_j} = \frac{\partial}{\partial x_j} \left[\left(\nu + \frac{\nu_T}{\sigma_\varepsilon} \right) \frac{\partial \varepsilon}{\partial x_j} \right] + C_{\varepsilon 1} \frac{\varepsilon}{k} \tau_{ij} \frac{\partial U_i}{\partial x_j} - C_{\varepsilon 2} \frac{\varepsilon^2}{k} \qquad \text{(Eq. 7)}$$

The turbulent viscosity is given by

$$\nu_T = C_\mu \frac{k^2}{\varepsilon} \qquad \text{(Eq. 8)}$$

CROSSFLOW FILTRATION EXPERIMENTS

A series of tests were performed to obtain filter flux results at two different scales with a Hanford tank simulant [2] The tests were made at the laboratory-bench scale on a cold (i.e., designated for non-radioactive simulant test materials) Cells Unit Filter (CUF) and in the Pretreatment Engineering Platform (PEP). PEP has up to 276 times the filter area available in CUF. One set of tests was conducted with the simulant feed (low solids) and one test was conducted at a relatively high solids concentration.

To facilitate the analysis of system scaling, CUF and PEP operations were designed to be equivalent. Both systems use similar filter elements (Mott sintered stainless steel filter tubes of 0.5-inch inner diameter) taken from the same manufacturer's lot. Both test configurations were similar – a filtration loop is fed from a slurry reservoir/tank with the filtration loop being composed of a slurry pumping system, filtration area, permeate collection and metering systems, heat exchanger (to remove mechanical heat), and filtration-loop backpressure valve.

SIMULATION RESULTS

A stochastic reconstruction of the pore-scale geometry for a section of the Mott sintered stainless steel filter tube was created based on available information. A filter wall porosity of 25% is assumed. Grain shapes and size distributions are estimated from two micrographs of inside and outside filter tube surfaces. The eight grain shapes used for the initial reconstruction are ellipsoids having diameters ranging from 6 to 22 microns and aspect ratios ranging from 1.0 (spherical) to 1.67. A wall thickness of approximately 200 microns was reconstructed, including the upstream filter wall face. Maximum and minimum dimensions measured for a sampling of the filter tubes used in the PEP experiments suggest an average wall thickness of roughly 1.8 mm, so approximately 11% of a filter wall thickness was included in the digital geometry. The column of material representing the small section of the filter wall is 80 microns in the axial and radial directions. Periodicity is assumed on the vertical faces. The initial reconstruction includes 1749 grains, and is shown in Figure 2. The granular character of upstream filter wall surface is visible on the top of the geometry.

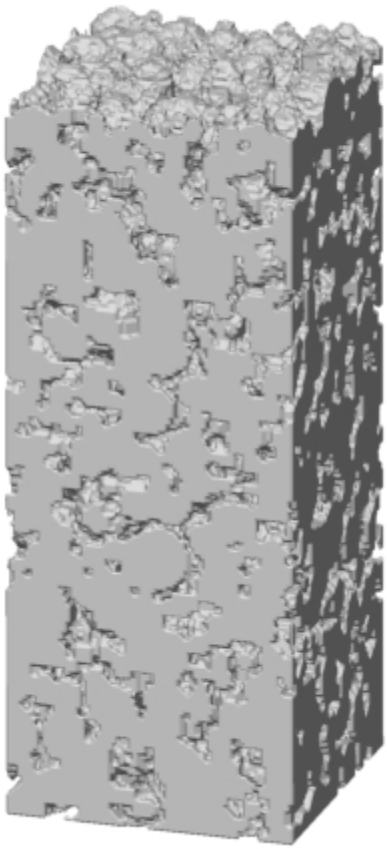

Figure 2. Reconstructed geometry for tube filter material.

A number of techniques could be applied to improve the fidelity of the digital reconstruction. Data on pore size distribution can be collected using techniques such as mercury porosimetry. Filter samples may be potted in epoxy, sectioned, polished, and micrographed in order to provide detailed images of internal pore structure. Statistical metrics such as chord length distributions[17] or two-point correlations may then be collected and used to compare the reconstruction to the real material. Grain sizes and shapes can be adjusted along with grain overlap in order to match the statistical 'fingerprints' collected from the micrographs of the filter wall cross-sections.

Details of the discrete particle filtration simulation are given in Table1. The domain extends 320 lattice spaces in the vertical direction, which gives a headspace of approximately 120 microns above the 200 micron thickness of filter media shown in Figure 2. Fluid flows downward through the column of filter media. Specified pressure boundaries are used on both the upstream and downstream faces of the domain. The specified pressure difference between the upstream and downstream faces corresponds to the normal trans-membrane pressure of 40 psid used in the PEP tests, scaled by the fractional thickness of the filter wall included in the simulation domain. Flow through the upstream boundary is assumed to be in a direction normal to the plane, so axial flow down the filter tube is not considered in the initial simulation. If particle momentum effects

were important during depth filtration, axial particle momentum may have some effect on the depth of particle penetration into the wall. Periodic boundaries are used on the vertical faces. The fluid is initially at rest, and is accelerated toward the filter wall by the pressure differential. The assumed particle specific gravity of 3.0 corresponds roughly to boehmite which makes up a large fraction of the insoluble solids in the PEP tests and is somewhat heavier than gibbsite, which is the other major component.

Table 1. Parameters for Pore-scale Filtration Simulation

domain dimensions	80 x 80 x 320
lattice spacing	1 μm
timestep for LB flow field solution	8.194E-8 s
timestep for particle tracking	1E-6 s
fluid temperature	298 K
fluid density, ρ	1,180 kg/m^3
fluid viscosity, μ	2.4 cP
LB relaxation parameter, τ	1.0
pressure on upstream face	30.0 kPa
pressure on downstream face	0.0 kPa
particle concentration	2.54E+11 1/cm^3
particle diameter	0.3 μm
particle density	3,000 kg/m^3
capture probability	0.1

When the solids-bearing fluid is initially drawn toward the filter surface, some particles penetrate through pore throats and into the interior of the filter wall. This process is often described as "depth filtration", as opposed to "cake filtration", which takes place only on the surface of the filter wall. During depth filtration, the total resistance to flow increases non-linearly and at a high rate per mass of particulate matter deposited. This happens because the particulate mass is accumulating in pore throats, where the fluid velocity is much higher than at the surface of the filter wall. Because the rate of particle removal is a function of particle concentration, which decreases as the fluid moves into the filter material, the rate of accumulation drops exponentially moving from the filter surface into the interior of the wall. Since the rate of accumulation is greatest in the pore throats at the upstream surface of the filter wall, these are quickly blocked, ending depth filtration and causing a transition to cake filtration. At this point, the total resistance to flow begins to change at a somewhat slower rate, since particulates are being collected at the filter wall surface, where local fluid velocities are lower. In practice, the transition from depth to cake filtration is not instantaneous, since it is a description of the aggregate behavior of flow paths and pore throats having a distribution of sizes. Once the pore throats are blocked, the pore mouths fill with solids. Eventually the roughness of the filter wall surface is obscured and additional accumulation happens in relatively flat layers. In the cross-flow filters to be employed in the WTP facility, the balance between competing rates of deposition and erosion quickly take over as the dominant factors governing the rate of cake growth.

Figure 3 shows accumulated solids deposits predicted by the micro-scale simulation at a point in time after all of the pore throats at the filter wall surface have become blocked. Filter solids are shown in red, and the filter substrate is semi-transparent. It can be seen that some limited solids penetration has taken place to a depth of approximately half of the thickness modeled, or roughly 100 microns. While narrow throats near the filter wall surface have been blocked, the mouths of the pores have not yet been completely filled with solids.

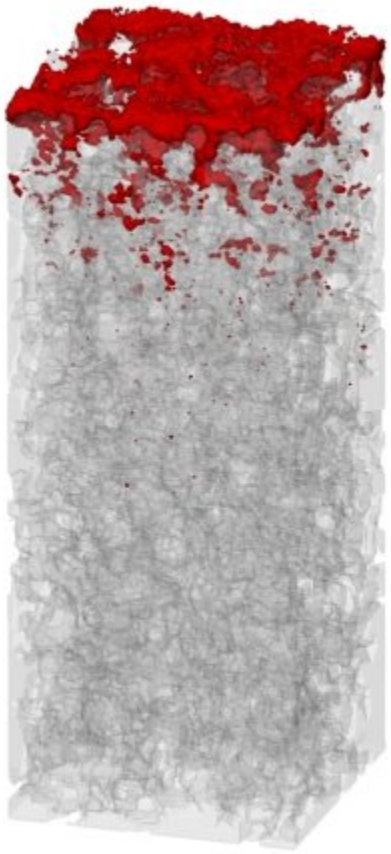

Figure 3. Accumulated solids deposits predicted by the micro-scale simulation

A transient device-scale simulation was performed for the initial 12 hours of the low-solids scaling test of the Pretreatment Engineering Platform (PEP) filter units. Assuming that the inlet development region is small and that the filtrate flux behaves linearly with the trans-membrane pressure, the filter unit is represented by a quarter-section of filter tube with periodic boundary conditions in the axial direction. The tube cross-section is divided into 0.0025 cm nodes, resulting in 635 node increments along the radius of the tube. The surface of the filter cake was modeled using a phase-field representation that tracks the surface as it moves through the computational grid.

The axial pressure drop was continuously adjusted to give an average tube velocity of 15 ft/s. The trans-membrane pressure drop was held at 40 psid. The permeate density for the test was 1.18 g/cm3 and the solids loading was continuously adjusted to give 6.9 wt% in the suspension

region and a specified particle size distribution.

The device-scale model filtrate flux results are presented in Figure 4 along with the measured fluxes for the five PEP filter units. The agreement is well within the variance of the filter unit data. The transient can be divided into three regions, as shown in the figure. At the start of the transient, the transverse flow convects the smaller particles into the filter tube matrix, where they are trapped. The increased flow resistance acts to slow the filtrate flux through the tube membrane. In addition, the particles larger than the pore openings concentrate near the filter surface and begin to form a concentration profile that creates a shear-induced back diffusion, slowing the flux rate of particles toward the filter surface.

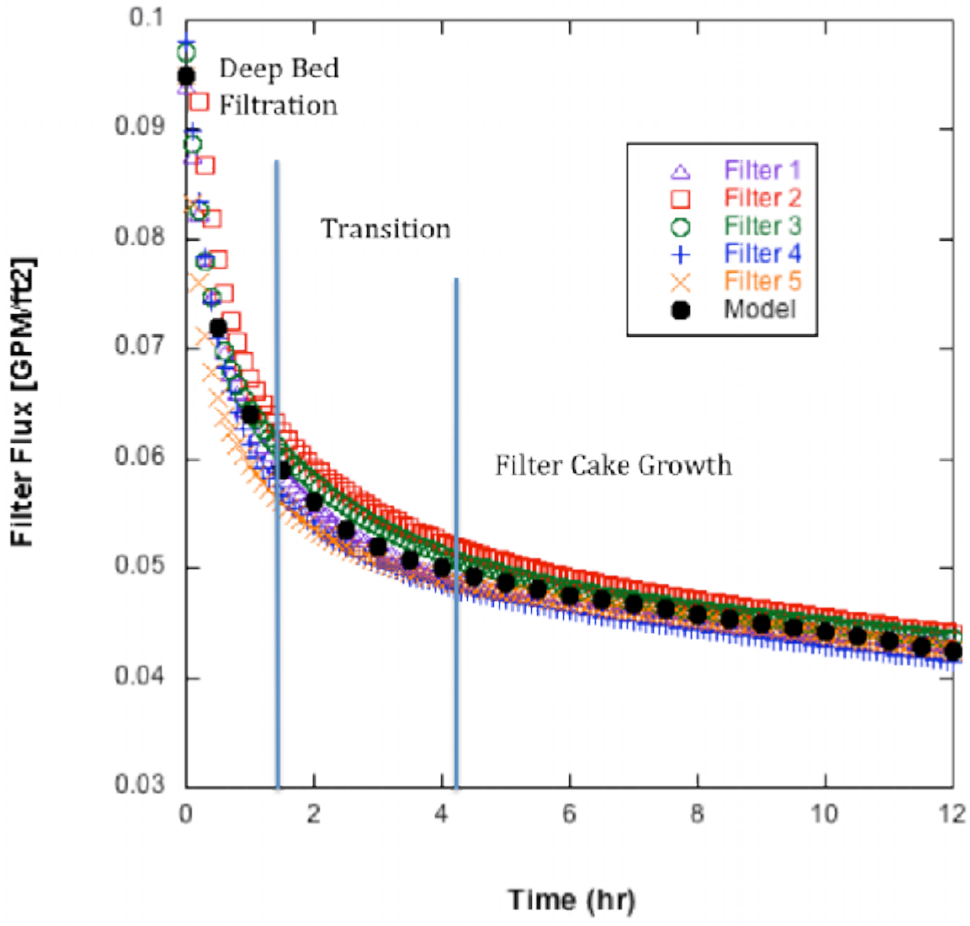

Figure 4. Comparison of filtrate flux model results with data curve fits for the five PEP filter units as a function of time.

The pores at the surface of the tube membrane have a distribution of throat sizes and flow rates, so that the time to fill or cover the pore throats with solid particles varies. The transition from deep-bed filtration to filter cake growth consists of the progressive blocking of different size pores, until all the pore openings have been covered with solid particles. The particle deposition from that point on contributes to the growth of the filter cake. The shear-induced back-diffusion preferentially transports the larger particles toward the center of the channel. Therefore, the particle size composition of the filter cake will be shifted to smaller diameter particles than the specified inlet particle size distribution.

CONCLUSIONS

A new simulation tool has been developed for modeling the flow and thermal performance of chemical processes that involve multiphase, chemically complex flows. This capability was demonstrated by modeling the ultrafiltration process which will be used in conjunction with leaching operations in the Hanford Waste Treatment Plant pretreatment facility. A pore-scale filter simulation was used to explore the nature of depth fouling and provide an indication of the maximum depth of particulate penetration into the filter wall. A device-scale filter model was able to match flux behavior observed in pilot scale ultrafilter experiments.

REFERENCES

1. WTP Project Doc. No. CCN 132846 “Comprehensive Review of the Hanford Waste Treatment Plant Flowsheet and Throughput-Assessment Conducted by an Independent Team of External Experts,” March 2006.

2. Daniel, R.C. et al. (2009). “EFRT M-12 Issue Resolution: Comparison of Filter Performance at PEP and CUF Scale”, WTP-RPT-185, PNNL-18498, Pacific Northwest National Laboratory, Richland, WA.

3. Geeting, J.G.H., R.T. Hallen, R.A. Peterson (2005). “Otimization of ultrafilter conditions using classical filtration models.” J. Membr. Sci. 265: 137-141.

4. Geeting, J.G.H., R.T. Hallen, R.A. Peterson (2006). “Ultrafilter Conditions for High-Level Waste Sludge Processing.” Sep. Sci. Tech. 41: 2313-2324.

5. Peterson, R.A., J.G.H. Geeing, R.C. Daniel (2007). “Estimation of Ultrafilter Performance Based on Characterization Data.” Chem. Eng. Tech. 30:1050-1054.

6. Filippova, O. and D. Hanel, Lattice-Boltzmann simulation of gas-particle flow in filters. COMPUTERS & FLUIDS, 1997. 26(7): p. 697-712.

7. Konstandopoulos, A.G., E. Skaperdas, and M. Masoudi, Microstructural Properties of Soot Deposits in Diesel Particulate Traps. SAE, 2002. 2002-01-1015.

8. Konstandopoulos, A.G., N.D. Vlachos, and G.N. Patrianakos, Application of Digital Material Methods to Silicon Carbide Diesel Particulate Filters. SAE 2007 World Congress, 2007. 2007-01-1131.

9. Yamamoto, K., et al., Lattice Boltzmann simulation on porous structure and soot accumulation. Mathematics And Computers In Simulation, 2006. 72(2-6): p. 257-263.

10. Kuwabara, S., The Forces experienced by Randomly Distributed Parallel Circular Cylinders or Spheres in a Viscous Flow at Small Reynolds Numbers. Journal of the Physical Society of Japan, 1959. 14(4): p. 527-532.

11. Konstandopoulos, A. and J.H. Johnson, Wall-Flow Diesel Particulate Filters - Their Pressure Drop and Collection Efficiency. SAE, 1989. 890405.

12. Elimelech, M., *Particle deposition and aggregation : measurement, modelling, and simulation*. Colloid and surface engineering series;. 1995, Oxford [England]: Boston. xv, 441 p.

13. Leighton, D. and A. Acrivos (1986). "Viscous Resuspension." Chem. Eng. Sci., 41(6): 1377-1384.

14. Shauly, A., A. Wachs, A. Nir (1998). "Shear-induced particle migration in a polydisperse concentrated suspension." J. Rheol. 42(6): 1329-1348.

15. Shauly, A., A. Wachs, A. Nir (2000). "Shear-induced particle migration in settling polydisperse concentrated suspension." Int. J. Mult. Flow. 26: 1-15.

16. Krieger, I.M. (1972). "Rheology of monodisperse lattices." Adv. Coll. Int. Sci. 3: 111-136.

17. Roberts, A. and S. Torquato, Chord-distribution functions of three-dimensional random media: Approximate first-passage times of Gaussian processes. PHYSICAL REVIEW E, 1999. 59(5): p. 4953-4963.